

1. Add co-ordinate system to all figures and use consistently with all equations.
2. Grammar + Wording needs major revisions, in section 8.4, ↗ as labelled + annotated,  
 ↗ In particular, 'reality' 'expected' and 'error' need be  
 be properly explained in the right order... I don't  
 think 'error' is even hinted at until the end of  
 the section. → I'd make 8.4 shorter and  
 present fundamentals and an order of magnitude estimate,

And define what you mean by  $z=0$ .  
 - I think  $z=0$  is the centre of the light sheet.

## Chapter 8

# Diffraction limited single virion tracking in SPIM

## 8.1 Introduction

✓ Herpesviruses are among the most complex and largest of the clinically relevant viruses and establish life-long infections in their hosts. They are widespread in vertebrates and humans, with up to 85% of the population worldwide being infected by herpes simplex virus 1 (HSV-1) and around 25% by HSV-2. Herpes simplex virus type 1 (HSV-1) is the most extensively studied herpesvirus, and is a general model for other alphaherpesviruses. Infections by the nine known human herpesviruses are associated with many serious diseases including certain lymphomas and life-threatening conditions in immuno-compromised patients [?]. Viral infections begin when infectious virus particles (virions) invade the organism by attaching to and entering susceptible cells. The virus hijacks the cellular machinery to replicate and produce progeny virus particles which then spread further infection. Herpesviruses pass through two distinct stages in their life cycle: lytic replication and latency.

Not much is known about the later stages of the infection cycle, the assembly of virus particles and their egress from the cell. Assembly and egress of viruses are essential stages in the herpesvirus lytic replication, hence contributing directly to pathogenesis, so imaging these

processes ~~processes~~ in particular is ~~an~~ an important goal of biomedical research.

Does not connect well from prior sentence.  
 Try: "Among the key steps within the lifecycle these stages, much remains to be learned about (a) the late stages of infection..."

### 8.1.1 Herpesvirus structure

In herpesviruses, the DNA genome is packaged in a nucleocapsid which is enveloped by a lipid membrane containing many viral membrane proteins. Nucleocapsid and envelope are separated by a complex, proteinaceous matrix called the tegument. The capsid is built up by the capsomers (capsid proteins) and possesses an icosahedral symmetry [? ]. The tegument is a densely packed protein layer around the nucleocapsid, and essential for structural integrity and functionality of the virion. While the nucleocapsid structure and protein composition is well understood, much less is known about the structure and assembly of the tegument. The tegument can be divided into inner tegument (capsid-associated part) and outer tegument (envelope-proximal part). For HSV-1, more than 20 viral tegument proteins are known [? ? ]. Most of these tegument proteins possess multiple functions aiding in the entry of viruses into the cell; transport of incoming nucleocapsids to the nuclear pore and genome release; as well as nuclear assembly and egress; nucleocapsid maturation and directed release from the cell. Contained in the viral envelope of HSV-1 are at least 11 glycoproteins as well as several membrane-associated proteins which play important roles in viral entry and egress as well as virus-induced cell fusion [? ? ].

### 8.1.2 Herpesvirus infection cycle

To initiate infection, herpesviruses first bind to cellular surface proteins which act as virus receptors. Due to direct fusion to the plasma membrane or endocytosis [? ], the viral capsid is delivered into the cytosol. Incoming capsids move towards the nuclear pore complexes by exploiting microtubules within the cell [? ? ]. There, they release the viral DNA through the nuclear pores into the nucleus [? ]. Virion proteins drive the initial transcription to produce mRNAs. Translation of these early mRNAs promotes further phases of viral gene transcription and replication of the viral DNA. Replication of the viral DNA is achieved through actions of viral polymerases and other viral replicative machinery. These replicated DNAs are used as templates for

Refer to  
Fig 8.1  
from  
Somewhere...

This seems like a good description of structure. But what are the question(s) that could be solved by imaging? End the note 8.1.1 by stating these.

The capsid then releases

is this  
active or passive  
transport?

If it's thought  
to make use of  
cellular transport  
systems, and moves  
along microtubules  
to the nucleus

## 8.2 Single Particle Tracking

93

late mRNAs, which produce viral structural proteins, and are also packaged into capsids late in infection [? ]. The egress pathway follows four steps (Figure 8.1):

1. Capsid assembly and genome encapsidation in the nucleus,
2. Primary envelopment and de-envelopment at the nuclear envelope,
3. Tegumentation and secondary envelopment in the cytoplasm,
4. Exocytosis at the plasma membrane or cell-to-cells spread at cell junctions.

In the nucleus, the capsid proteins coassemble autocatalytically with and around the *portal complex* in late infection [? ]. After capsids are formed and packaged in the nucleus, the capsids traverse the nuclear envelope. The nuclear envelope consists of a double membrane, the inner and outer nuclear membranes (INM, ONM). The capsids bud into the INM (primary envelopment) to form an enveloped particle in the perinuclear space, fuse with the outer nuclear membrane (de-envelopment) and are released into the cytoplasm [? ]. In the cytosol, the capsids associate with more tegument proteins and bind onto and bud into cytoplasmic membranes derived from endosomes and/or the trans-Golgi network (secondary envelopment) [? ? ]. Although details of the mechanisms are not well understood, tegument maturation is likely directly connected to secondary envelopment via direct protein-protein interactions. Enveloped virions are finally secreted from cells by exocytosis [? ? ].

## 8.2 Single Particle Tracking

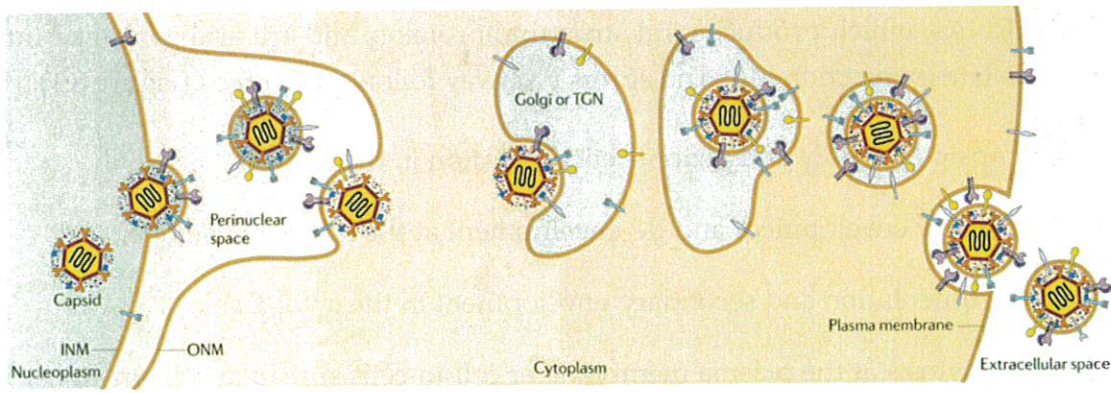
MICROSCOPY.

Lateral

While optical imaging is generally limited to a resolution of ~250 nm nm by diffraction, sparse emitters can be localised with much higher precision by fitting a model function to their intensity distribution. Tracking individual particles is an important tool for modern biology. It has been used to study intracellular transport such as the movement of mRNA[? ]; cell membrane dynamics[? ] and more. Many studies exist on inter and intra cellular viral trafficking using single particle tracking [? ]. Only a few and recent works exclusively probe the molecular egress pathway of herpesviruses. Hogue *et al.* [? ] used total internal reflection fluorescence (TIRF) microscopy to selectively visualise fluorescent Pseudorabies viruses near the plasma membrane and follow them during exocytosis. Sandbaumhüter *et al.* showed, by a motility analysis of fluorescent HSV-1, that directed transport of cytosolic capsids

intercellular and intracellular

and ...  
by observing the  
motion of membrane-bound  
particula



Nature Reviews | Microbiology

Fig. 8.1 Scheme of assembly and egress pathway of virus particles. After capsids are formed in the nucleus, they bud into the inner nuclear membrane (INM) (primary envelopment) to form an enveloped particle in the perinuclear space. These particles fuse with the outer nuclear membrane (ONM) (de-envelopment) and are released into the cytoplasm, leaving the envelope in the ONM. In the cytosol, capsids bind onto and bud into cytoplasmic membranes (secondary envelopment), and enveloped virions are secreted from cells (release). Figure from [? ].

1 was dependent on both tegument proteins pUL36 and pUL37 [? ]. Virus trafficking  
2 and how viruses penetrate the nucleus of a cell have also been studied using SPT [? ].

3 Due to a limited depth of field, particles tracked in a 3D volume tend leave the  
4 axial detection range. Several technical approaches already exist to perform SPT in  
5 three dimensions [? ]. Orbital tracking in two planes was applied to track prototype  
6 foamy virus (PFV) in real-time inside cells [? ], and a rotating, oblique light sheet and  
7 astigmatic detection were used to image and track viral capsids with high temporal  
8 and spatial resolution inside the cell nucleus [? ].

Basically,  
I want to  
avoid the  
term  
"deconstruct"

### 8.2.1 Particle spatial localisation

[TRACKING]

define a particle tracking  
method as consisting of the  
following steps:

[DETECTION]

Particle tracking can be broadly described as a two stage process, spatial localisation  
then temporal localisation. Crocker *et al.* deconstructed the problem into logical  
computable steps. Each image is corrected for any distortion or error from the  
digitation process, as well a de-noising step. Pixels with local maximum brightness  
are identified as candidate particles and compete with other candidates within a  
pre-defined radius slightly larger than the expected size of the particle. A centroid  
(centre of mass) fitting procedure is employed under the assumption that, spherical  
emitters can be well-defined by a Gaussian profile. By fitting a Gaussian profile

POINT-LIKE PARTICLES WITH SYMMETRIC IMAGES ARE BEING OBSERVED  
followed by bandpass filtering to  
suppress image noise.

I think Crocker uses  
centroid = centre of mass,  
not Gaussian... PTA

SECOND,  
local pixel  
value maxima  
(or minima,  
depending on  
the nature of  
the particle  
tracking  
problem)

Key Thing  
1. End this  
section  
8-2-0  
by saying  
what you  
will do.

2. Describe  
the terms  
underlined in  
red, using  
natural  
language.

3. Are these  
literature  
techniques?

If so:  
"they  
have been done"

If they are your methods,  
write that they "will be used" in this project.

even  
or even the particle image's centre of mass in simple cases)

Draft - v1.0

Friday 1<sup>st</sup> June, 2018 – 17:50

### 8.3 Astigmatic tracking

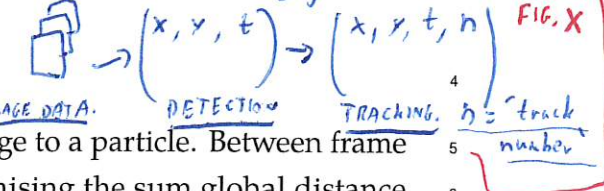
95

particulate positioning can be recorded with sub-pixel accuracy. Typically iterative least squares fitting is used due to its ease of implementation, speed, precision and robustness.

e

inferred/recovered/estimated

should be titled "particle detection", and "8.2.2" should be "particle tracking". I think. Consider a figure to illustrate:



#### 8.2.2 Particle temporal localisation

Temporal localisation refers to the assignment of lineage to a particle. Between frame 1 and 2, particulate identity is determined by minimising the sum global distance between particles at each time point. By frame 3, momentum can be assigned to a particle as well to decrease the chance of two path identities being falsely merged or switched. The same applies for acceleration and higher order speed derivatives, but with a lessening of overall significance. The chance of a lineage being correctly assigned largely relies on the sampling rate of the imaging, with higher rates being favourable.

#### 8.2.3 Light sheet single particle tracking

Spille et. al. proposed using light-sheet microscopy for tracking particles over long periods. This was achieved by shifting their light-sheet and detection objective at each recorded frame such that the particle was repositioned to the centre of the sheet. Alternatively, the entire sample could be relative to a static sheet. Spille demonstrated this technique very successfully on a single molecule of mRNA (50nm[?]) moving on the membrane of a nucleus[?] (see Figure 8.2).

Particle tracking results within the image data stack were then combined with information about the movement of the imaging volume to return estimates of particle movement within the specimen.

### 8.3 Astigmatic tracking

To successfully reposition the light-sheet for axial particle tracking, precise axial localisation (within the sheet) is needed. Adding a weakly cylindrical lens within the detection optics will add astigmatism to the point spread function of the microscope.

The asymmetry in focal lengths in the imaging plane axes means that along one axis the focal point will be offset axially compared to the orthogonal axis. The result is that there is an overall axial asymmetry in the detection PSF, for point sources this allows axial position to be encoded in the recorded image. This technique was used to great effect in dSTORM and PALM systems, which rely on the localisation of point emitters to create 3D volume super-resolution images [ ]. The range over which a

Show in  
Figure, (8.2e?)  
to explain.

If it is the  
design used in this  
project, say so more  
clearly.

Problem:  
IS THIS  
WHAT  
I DID?  
OR  
WHAT  
COULD BE  
DONE,  
BASED ON  
LITERATURE.

Reward.

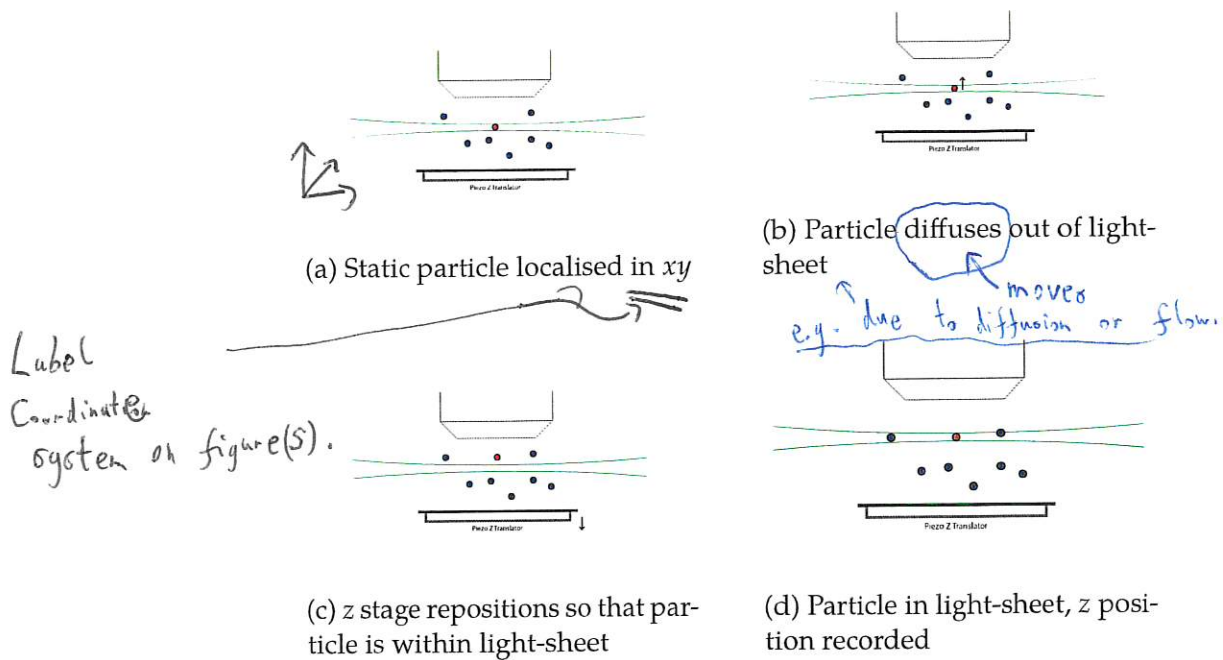


Fig. 8.2 Routine to track particles three dimensionally using light-sheet.

- <sup>1</sup> cylindrical lens can axial encode is at most  $\sim 1 \mu\text{m}$ , before the non-linearity in the
- <sup>2</sup> astigmatism becomes too great and the PSF is too blurred to fit computationally.

### 8.3.1 Axial localisation

In a typical 3D localisation workflow, the position of the emitter is first localised laterally in 2D, and then axially.  
 Assuming an accurate localisation in 2D, the image of the point emitter is then localised axially. With each of the methods presented here, a monotonic calibration volume of known distance is needed.

#### 7 Gaussian fitting

- The ratio of the (FWHM) of the Gaussian along the major and minor axes will produce a calibration curve for axial position. The major and minor axis sigma values are obtained by fitting a 2D Gaussian function to the rotated and centered point image. However, this technique is computational expensive and slow techniques to recover axial position is fitting a 2D Gaussian. Attempting an iterative 2D Gaussian fitting in real-time is unrealistic with current computing capabilities, as such this technique is only useful in passive analysis of images already recorded.

post-capture analysis (?)

## 8.3 Astigmatic tracking

97

Template matching

Have a 1<sup>st</sup> sentence: cross-correlation is...  
 Then this seems like a second sentence,

Cross-correlation requires no fitting step and scales in computational complexity with the image as  $O(n^2)$ . As such using fewer pixels to recover axial position allows this technique to function in real-time. The cross correlation of two signals returns a single value representing an unnormalised similarity of the two signals. Provided the astigmatism is transitioning linearly, a cross-correlation for every image in the calibrated stack may not be needed. By using all the images in the calibration stack, the computational time increases by the half the number of axial images in that stack. The ratio of the cross correlation of two images spaced axially and equally about the focal centre of the stack will give an estimate of particle position. This estimate is sufficient for real-time results; and provided the images of the point-emitter are recorded, a more accurate axial localisation step can be applied in post-analysis. The discrete cross-correlation function:

 $(f * g)$ 

$$(f * g)[n] \stackrel{\text{def}}{=} \sum_{m=-\infty}^{\infty} f^*[m] g[m+n] \quad (8.1)$$

$\nwarrow$  WHAT DOES THE  $*$  OPERATOR MEAN? DEFINE.

Similarly the covariance of the calibration an image or volume can be used, though the computational complexity is lower again.

$$\text{cov}(X, Y) = \frac{1}{n} \sum_{i=1}^n (x_i - E(X))(y_i - E(Y)) \quad (8.2)$$

$$= \frac{1}{n^2} \sum_{i=1}^n \sum_{j=1}^n \frac{1}{2} (x_i - x_j) \cdot (y_i - y_j) \quad (8.3)$$

8.3.2 Simulations of image data to test particle tracking methods

To verify that single particle tracking in light-sheet microscopy was possible, the diffusion of a single diffraction limited particle was simulated *in silico* (see Figure 8.3). To create the simulation, the particle was modelled to take a random walk of time steps  $dt$  across a single imaging exposure of 40 ms. This simulated how the particle would appear to move within the light-sheet. The intensity of the final image of a particle was attenuated according to the Gaussian intensity of the light-sheet axially ( $z$ ) and laterally ( $x, y$ ) as per:

$dt \approx 0.1 \text{ ms}$

$\nwarrow$  To simulate dynamic blur.  $\uparrow$  do its position varied within the Gaussian light sheet  $\uparrow$  Illumination  $\uparrow$  (during each frame acquisition, creating 'dynamic blur' as described by Savin and Doyle.)

The problem is that

you are actually defining a forward model of the image formation, which = (Illumination Intensity)  $\otimes$  (response function)

but you describe 'attenuation' as if you are fixing an over-simplified model rather than

Make sure  
co-ordinate system  
in Fig 8.3 is  
consistent with  
Fig 8.2 and  
the rest of  
the chapter.

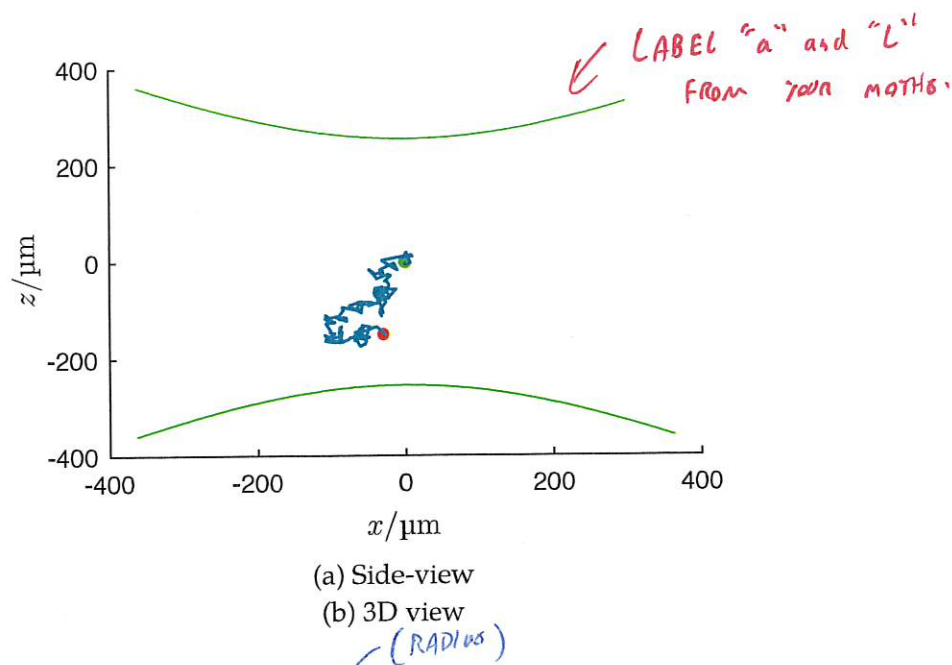


Figure 8.3, but needs complete caption! { Fig. 8.3 Simulations of a single particle diffusing within a light-sheet with a viscosity of 25% glycerol in water in a Newtonian fluid medium with a viscosity of XXX (as 25% glycerol in water). Particle track length corresponds to 40 ms of real time. Temperature = .

$$w_0 = 1.4 \lambda \frac{NA}{n} \quad (8.4)$$

$$w(y) = w_0 \sqrt{1 + \left(\frac{y}{y_R}\right)^2} \quad (8.5)$$

$$y_R = \frac{\pi w_0^2}{\lambda} \quad (8.6)$$

$$I(x, y, z) = I_0 \left( \frac{w_0}{w(y)} \right)^2 e^{-2 \frac{z^2}{w(y)^2}} \quad (8.7)$$

Where  $w_0$  is the beam waist; NA is the numerical aperture of the excitation objective,  $n$  is the refractive index of glass;  $\lambda$  is the wavelength of excitation light;  $y_R$  is the Rayleigh length and  $w(y)$  is the beam waist through  $y$ .

Ok, but see my comments about ~~the~~ the image formation model.

## 8.4 Motion-induced astigmatic axial localisation error

**Some motion-blurred images are elongated in a way that implies can give position estimator.**

(and in Savin + Doyle paper.) So that its image which can resemble an the elongated image of a

It was demonstrated in the computational simulations that a particle moving in a real system will demonstrate a motion blur unique to having astigmatism. A single particle moving quickly in  $xy$  will appear to stretch and the localised position of the particle will be the average of the start and end position. With astigmatism, the image of particle does not vary linearly with the distance the particle has travelled axially during that epoch. This response was modelled using a false astigmatism to emulate an approximate response of the system. //A Gaussian was convolved with the single point in space, with the assumption that the depth of field of the detection objective was longer than the width of the light-sheet and that intensity across the sheet was uniform; the latter assumption is invalid, but a varying intensity only controls the SNR across the sheet. A Gaussian function being used to model a particle is a valid assumption as Gaussian models are used in the fitting process for localisation from the pixel data.

To astigmatically narrow the Gaussian as the particle moved through  $z$  the standard Gaussian equation of:

$$f(x, y) = e^{-\frac{x^2+y^2}{\sigma^2}} \quad (8.8)$$

2 $\sigma^2$  or  $\sigma^2$ . 2 $\sigma^2$  gives std. deviation  $\sigma$  or second central moment  $\sigma^2$ .

was modified to use a simple model of astigmatism by assuming assume that  $\sigma$  depends on  $z$  such that:

describes the

Prefer

$$\sigma(z) = kz + c$$

This implies  $\sigma = 0$  at some  $z$ ... Wrong!

$$\sqrt{\frac{1}{k^2(z+c)^2} + \sigma_0^2}$$

Where  $k$  is an arbitrary degree of astigmatism and  $c$  is the particle size when there is no astigmatism. We can then redefine  $k$  in terms of  $a$ , where  $a$  is a function of  $c$  and  $L_{end}$ , with  $L_{end}$  being the distance the particle will be when the Gaussian is  $\frac{1}{a}$  narrower:

$$k = \frac{ac}{L_{end}}$$

I don't understand this definition. (8.10)

the point spread function radius

This seems wrong.

Gaussian to model PSF ✓

Again. axial displacement of the particle It is useful to express  $k$  in terms of...

For Line 16-17:

$$\text{If } \sigma^2 = k^2 z^2 + c^2 = \left(\frac{a^2 c^2}{L_{end}}\right) z^2 + c^2$$

I THINK THIS DEFINITION IS WRONG BUT

$$\text{If } z=L_{end}, \sigma^2 = a^2 c^2 + c^2 \dots \text{what is } L_{end}?$$

$$z=L_{end} \rightarrow \sigma = \sqrt{1+a^2} \sigma \dots$$

Gaussian to model particle position X as real tracks are not, individually, Gaussian — they are random. ..."

- The negative gradient relationship then holds for the orthogonal dimension to give a full 3D model:

*for the PSF:*

$$f(x, y, z) = e^{-\frac{x^2}{kz+c} + \frac{y^2}{-kz+c}} \quad (8.11)$$

*bottom term should be  $2\sigma_x^2, 2\sigma_y^2$  where equations for  $\sigma_x, \sigma_y$  are from fixed variance of 8.9.*

- To make calculations tractable, all modelling was considered in  $xz$  as the effect of astigmatism in  $y$  is independent. By normalising the Gaussian model, we simulate that an equivalent number of photons are being emitted by the particle, this allows the expected and real PSFs to be compared.

Only estimates from data have a hat ( $\hat{x}$ ).  $\rightarrow \hat{\text{PSF}}_{\text{Expected}} = \underbrace{\frac{1}{\sigma(z)\sqrt{2\pi}}}_{\text{normalised}} e^{-\frac{x^2}{2\sigma(z)^2}}$

*Equation #6.*

$$\text{PSF}_{\text{Expected}} = e^{-\frac{x^2}{2\sigma(z)^2}}$$

*proportional to,*

*in the z-direction*

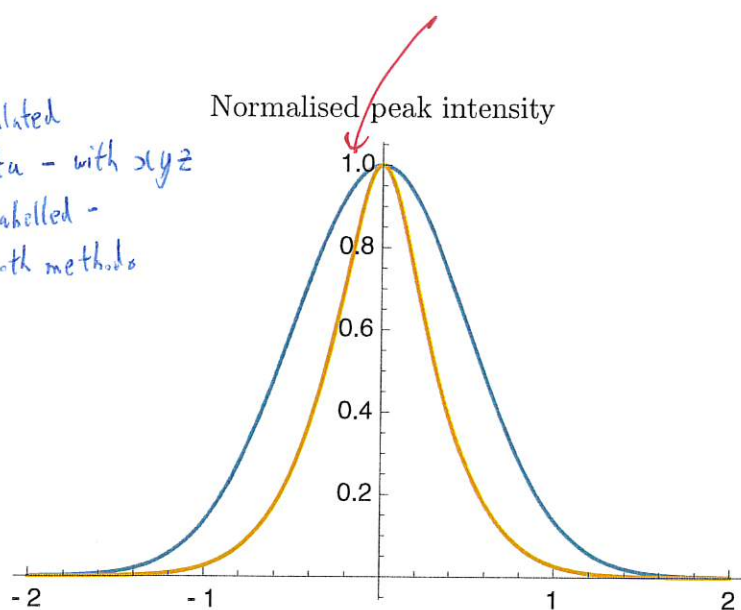
- Assuming that the particle moves a distance  $L$  with uniform speed and uniform emission of photons en-route, integrating the function gives the real PSF.

$$\begin{aligned} \hat{\text{PSF}}_{\text{Reality}} &= \frac{1}{L} \int_0^L \frac{1}{\sigma(z)\sqrt{2\pi}} e^{-\frac{x^2}{2\sigma(z)^2}} dz \\ &= \frac{L_{\text{end}} \left( \text{Ei} \left( -\frac{x^2}{2c^2} \right) - \text{Ei} \left( -\frac{L_{\text{end}}^2 x^2}{2c^2(L_{\text{end}}+aL)^2} \right) \right)}{2\sqrt{2\pi acL}} \end{aligned}$$

Where  $\text{Ei}$  is the exponential integral, readily evaluated computationally, as defined as:

I think both of these are models,  
So you can't call one 'real'  
 — 'Approximation'  
 — 'Numerical' might be two possible  
 subscripts to define this,

Figure: Give simulated image data - with xyz axes labelled - from both methods



I think units = Irradiance  
=  $\text{W/m}^2$  arriving at a surface.

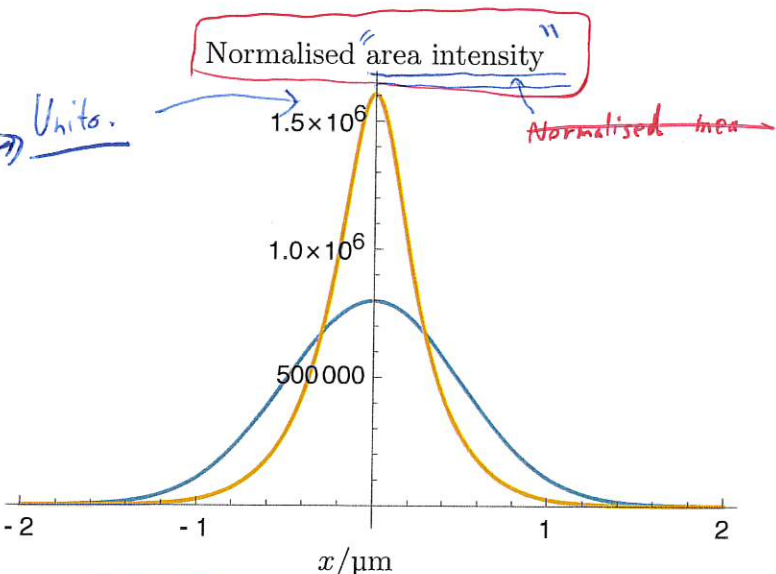


Fig. 8.4 a) Expected versus reality PSF profile of a particle using normalised peak intensity, a weaker model for astigmatism b) Uses normalised area of the Expected and Reality PSFs for a more accurate model of astigmatism

One is only 'Reality' if it was measured experimentally.  
Suggest: approximation + numerical if both are simulated.  
Also "Reality PSF" sounds horribly ungrammatical.

The integral has to be scaled by  $\frac{1}{L}$  as integrating a function over  $0 \rightarrow L$  will scale the total area by  $L$ . The resultant function is then comparable with  $\text{PSF}_{\text{Expected}}$ .

$$\begin{aligned} \text{PSF}_{\text{Reality}} = & \frac{2c(aL + L_{\text{end}})e^{-\frac{L_{\text{end}}^2 x^2}{2c^2(aL + L_{\text{end}})^2}}}{2acL} \\ & + \frac{L_{\text{end}}x\sqrt{2\pi}\text{Erf}\left(\frac{(L_{\text{end}}x)}{\sqrt{2}(acL + cL_{\text{end}})}\right)}{2acL} \\ & + \frac{L_{\text{end}}\left(2ce^{-\frac{x^2}{2c^2}} + \sqrt{2\pi}x\text{Erf}\left(\frac{x}{\sqrt{2c}}\right)\right)}{2acL} \end{aligned}$$

This is  
not generally  
true. True for  
a constant or  
fixed  $f(x)$ ,  
but with some  
defined constraints.

### 8.4.1 Cross correlation

To analytically compare the expected and real results, the respective functions were cross-correlated using the analytical function:

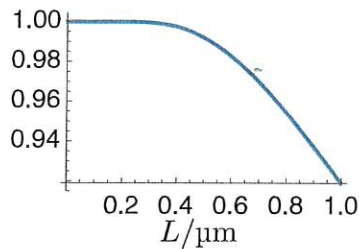
$$(f * g)(t) \stackrel{\text{def}}{=} \int_{-\infty}^{\infty} f(x)^* g(x+t) dx$$

The integral of the result across all space gives a single value signifying the quality of correlation between the two functions:

$$\int_{-\infty}^{\infty} \int_{-\infty}^{\infty} f(t)^* g(x+t) dx dt$$

This value will reach unity when  $f(x) = g(x)$

a) Normalised correlation



b) Normalised correlation

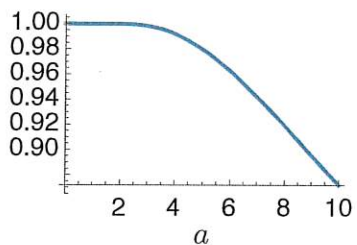


Fig. 8.5 CAPTION. WHAT PART OF THE MAIN TEXT POINTS TO THIS?

The expected PSF was given the additional  $t$  parameter as it was more likely that this integral would solve, though, this only solves across all space for unnormalised PSFs:

I don't follow this.

what would the integral solve?  
Do you mean  
be solvable?

$$\begin{aligned}
 & \int_{-\infty}^{\infty} \int_{-\infty}^{\infty} \text{PSF}_{\text{Reality}}(x)^* \text{PSF}_{\text{Expected}}(x+t) dx dt \\
 &= \frac{\pi c(aL + L_{\text{end}})^2}{aL_{\text{end}}L \sqrt{\frac{L_{\text{end}}^2}{c^2(aL + L_{\text{end}})^2}}} + \frac{2\pi c^2(aL + L_{\text{end}})^2}{L_{\text{end}}^2} \\
 &+ \frac{\pi cL_{\text{end}}}{aL \sqrt{\frac{L_{\text{end}}^2}{c^2(aL + L_{\text{end}})^2}}} - \frac{2\pi L_{\text{end}}}{a \sqrt{\frac{1}{c^2}} L \sqrt{\frac{L_{\text{end}}^2}{c^2(aL + L_{\text{end}})^2}}} \\
 &+ \frac{2\pi c^2(aL + L_{\text{end}})^2}{aL_{\text{end}}L}
 \end{aligned}$$

By correlating the normalised functions across a small window  $u$  an analytical solution was produced.

WHY HATS?

$$\begin{aligned}
 & \int_{-u}^u \int_{-\infty}^{\infty} \hat{\text{PSF}}_{\text{Reality}}(x)^* \hat{\text{PSF}}_{\text{Expected}}(x+t) dx dt \\
 &= -\frac{(aL + L_{\text{end}})}{\sqrt{2\pi aL_{\text{end}}L}} \sqrt{\frac{L_{\text{end}}^2}{c^2(aL + L_{\text{end}})^2}} \left( L_{\text{end}}u \left( \text{Ei} \left( -\frac{L_{\text{end}}^2 u^2}{2c^2(L_{\text{end}} + aL)^2} \right) + \Gamma \left( 0, \frac{u^2}{2c^2} \right) \right) \right. \\
 & \quad \left. - \frac{\sqrt{2\pi(-c)}(aL + L_{\text{end}}) \left( \text{Erf} \left( \frac{L_{\text{end}}u}{\sqrt{2}(acL + cL_{\text{end}})} \right) \right)}{\sqrt{2\pi aL_{\text{end}}L}} - \frac{\sqrt{2\pi}L_{\text{end}}|c| \text{Erf} \left( \frac{u}{\sqrt{2}|c|} \right)}{\sqrt{2\pi aL_{\text{end}}L}} \right)
 \end{aligned}$$

WHAT CONCLUSION DO YOU WANT TO MAKE?

IS IT: For particle speed < ~~10~~ (Some Value), axial localisation [position estimation] using equation [give exact equation number] was essentially correct if this in m precision; less precise at faster speeds due to motion blur?

## Grammar.

Do you mean of  $\hat{z}$ -position could be estimated by finding the calibration image data with known  $z$ -position that has the highest correlation with observed data? Friday 1<sup>st</sup> June, 2018 - 17:50

Draft - v1.0

104 2. - BUT SLOW  
3. Hence to get estimate of  $z$  from Gaussian fitted FWHM.  
Diffraction limited single virion tracking in SPIM

1 8.4.2 **GRAMMATICALLY INCOMPLETE**  
**Full width half maximum TO ESTIMATE AXIAL POSITION OF A PARTICLE.**  
**FITTING EVALUATIVE USING**

2 The correlation of two signals is not an absolute error which can be used to make predictions about real-world systems. So, the Full Width at Half Maximum of each of the two signals was considered as this property, in Gaussian-like functions, should provide an analogue for  $\sigma(z)$  which may be compared absolutely.

6  $\text{PSF}(x, \dots) - \lim_{x \rightarrow 0} \frac{\text{PSF}(x, \dots)}{2} = 0$

7  $\Rightarrow \text{FWHM}_{\text{Expected}} = 2x$   
8  $= \left| -\frac{\sqrt{2c}\sqrt{\ln 2 + 2i\pi n}(aL + L_{\text{end}})}{L_{\text{end}}} \right|, n \in \mathbb{Z}$

11  $\text{PSF}_{\text{Reality}}(x, \dots) - \lim_{x \rightarrow 0} \frac{\text{PSF}_{\text{Reality}}(x, \dots)}{2} = 0$

12 *Grammar.* This equation does not solve for  $x$  so a Maclaurin expansion was used: *Cannot be solved to give a closed-form expression for  $\sigma_z$ ,*

14  $= -\frac{L_{\text{end}}x^2}{4(c^2(aL + L_{\text{end}}))} + \frac{x^4(a^2L_{\text{end}}L^2 + 3aL_{\text{end}}^2L + 3L_{\text{end}}^3)}{48c^4(aL + L_{\text{end}})^3} + O(x^5)$

16  $\Rightarrow \text{FWHM}_{\text{Reality}} = \frac{2\sqrt{3}}{\sqrt{\frac{a^2L^2}{c^2(aL + L_{\text{end}})^2} + \frac{3L_{\text{end}}^2}{c^2(aL + L_{\text{end}})^2} + \frac{3aL_{\text{end}}L}{c^2(aL + L_{\text{end}})^2}}}$

18  $\text{FWHM}_{\text{Error}} = 2 \frac{\text{PSF}_{\text{Expected}} - \text{PSF}_{\text{Reality}}}{\text{PSF}_{\text{Expected}} + \text{PSF}_{\text{Reality}}}$   
19  $= 2 \frac{\sqrt{\ln 2} \sqrt{a^2L^2 + 3aL_{\text{end}}L + 3L_{\text{end}}^2} - \sqrt{3}L_{\text{end}}}{\sqrt{\ln 2} \sqrt{a^2L^2 + 3aL_{\text{end}}L + 3L_{\text{end}}^2} + \sqrt{3}L_{\text{end}}}$

SAY  
WHAT  
THIS IS  
USED FOR.  
DON'T FORGET  
GLOSSARY.

## 8.4.3 Area analysis

22 When  $L \rightarrow 0$  this result of  $\text{FWHM}_{\text{Error}}$  can be below zero, which would suggest  
23 that the result is not an accurate measure of the true error. This is likely due to the  
24 process requiring a series expansion, at  $x = 0$ ; as the series expansion is only an  
25 approximation of the target function. Since attaining error from the FWHM fails for  
26 small values of  $L$  an analysis using area was considered. For Gaussian-like functions

Obtaining?

WHAT DO YOU MEAN  
BY ERROR?

$z$ -position? Image mis-fit?

I think you talk  
about this on p.105-106 - useless!

Are you just looking

for a short expression for  
 $\hat{z}$  in terms of  $\hat{\sigma}_x, \hat{\sigma}_y$

the total area under the curve is proportional to  $\sigma(z)$ , so by comparing the area covered by the expected and real PSFs a valid measure of error could be obtained.

This analysis does not work for normalised PSFs as the area is unity in each case, as such the unnormalised model was used. Using an unnormalised function was still valid as the area was only being used as a proxy for finding a measure of the width of the PSF being interrogated.

$$\int_{-\infty}^{\infty} \text{PSF}(x, \dots)_{\text{Expected}} dx = \frac{\sqrt{2\pi}}{\sqrt{\left(\frac{acL}{L_{\text{end}}} + c\right)^2}}$$

$$\int_{-\infty}^{\infty} \text{PSF}(x, \dots)_{\text{Reality}} dx = \sqrt{\frac{\pi}{2}} \left( \frac{2(aL + L_{\text{end}})}{aL \sqrt{\frac{L_{\text{end}}^2}{c^2(aL + L_{\text{end}})^2}}} - \frac{2L_{\text{end}}}{a \sqrt{\frac{1}{c^2}L}} + c \left( -\frac{aL}{L_{\text{end}}} - 2 \right) \right)$$

$$\text{Error} = \frac{\int_{-\infty}^{\infty} \text{PSF}(x, \dots)_{\text{Expected}} dx - \int_{-\infty}^{\infty} \text{PSF}(x, \dots)_{\text{Reality}} dx}{\int_{-\infty}^{\infty} \text{PSF}(x, \dots)_{\text{Expected}} dx + \int_{-\infty}^{\infty} \text{PSF}(x, \dots)_{\text{Reality}} dx}$$

$$= \frac{2 \cdot \left( -\frac{2L_{\text{end}}}{aL \sqrt{\frac{L_{\text{end}}^2}{c^2(aL + L_{\text{end}})^2}}} + \frac{2L_{\text{end}}}{a \sqrt{\frac{1}{c^2}L}} + c \left( \frac{aL}{L_{\text{end}}} + 2 \right) \right)}{aL \sqrt{\frac{L_{\text{end}}^2}{c^2(aL + L_{\text{end}})^2}} - \frac{2L_{\text{end}}}{a \sqrt{\frac{1}{c^2}L}} + c \left( -\frac{aL}{L_{\text{end}}} - 2 \right)}$$

dot:

The above equation details how much error in width the astigmatism is expected to accrue over a length  $L$ . This length  $L$  may be computed from the three dimensional diffusivity of a small particle from the diffusivity  $D$ :

$$D = \frac{kT}{6\pi\mu r}$$

Do you mean 'if  
the particle's axial location  
changes by a displacement  $L$ ,  
at uniform velocity' during the  
image exposure time?

If so, you are at best  
obtaining an expression for the  
order-of-magnitude localisation error.

Astigmatism is not a person or  
entity than can 'accrue' anything.  
I don't know what word you are  
looking for! 'Cause'?  
And the

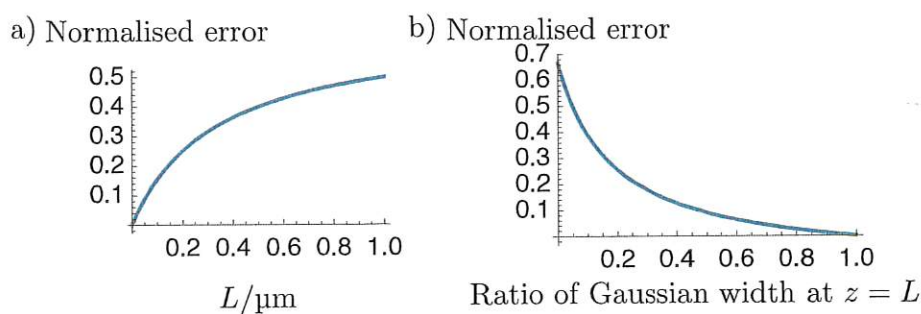


Fig. 8.6 a) Error was plotted against distance the particle travels in a single epoch b) The degree of astigmatism  $k$  was reframed such that it a substitute parameter represented the ratio of the width of the Gaussian at  $z = 0$  and  $z = L$ . This graph shows that as the ratio approaches unity the error due to astigmatic smearing becomes 0. However, when the ratio of the widths approaches 0, the error does not approach infinity as would be expected.

Where  $k$  is Boltzmann's constant,  $T$  is temperature,  $\mu$  is the viscosity of the medium,  $r$  is the radius of the particle, from  $D$  the average distance of diffusion  $w$  can be computed:

$$w^2 = q_i D t$$

Where  $q_i$  is the dimensionality of the diffusion and  $t$  is the time elapsed. By setting the parameters to realistic world values:  $T = 298 \text{ K}$ ;  $\mu = 0.002 \text{ N s m}^{-1}$ ;  $k = 1.3806 \times 10^{-23} \text{ m kg}^2 \text{s}^{-2} \text{K}^{-1}$ ;  $c = r = 100 \text{ nm}$ ;  $a = \frac{1}{5}$ ;  $L_{\text{end}} = 0.5 \mu\text{m}$ ; an average axial position error of 25.7% is observed.

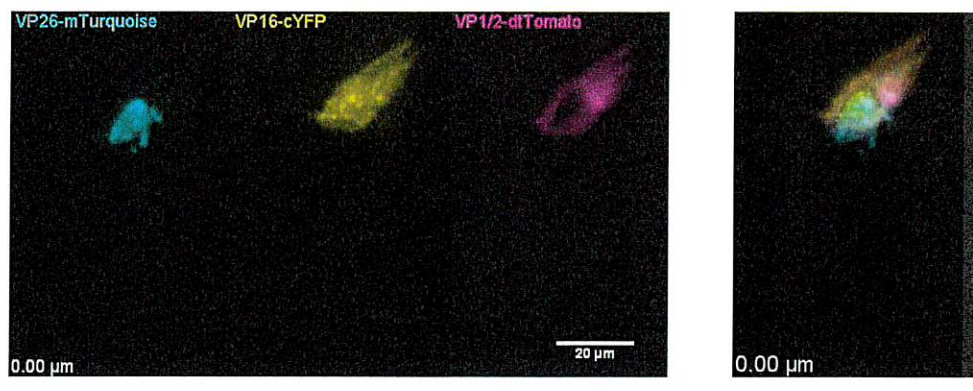
About 25 % caused by           

## 8.5 Results

### 8.5.1 Cellular imaging

As a proof of principle, virally infected HeLa cells were mounted and imaged using the modified light-sheet microscope. The cells were infected with HSV-1 expressing tegument proteins fused to fluorescent proteins (VP26-mTurquoise, VP1/2-dsTomato, VP16-cYFP). Trypsin was used to help lift cells in culture into solution and was left to act for 3 min. 10% Foetal Bovine Serum (FBS) was added to deactivate the Trypsin as it is a protease enzyme and will further degrade the cells. Coverslips were submerged in the cellular solution and left to adhere and culture on the glass. 3%

on         ?



(a) Separate colour channels

(b) Merged

Fig. 8.7 HSV-1 viral tegument proteins volumetrically imaged in fixed cells using a light-sheet microscope. [State what the VC26 etc. i.e. the different colour chan

## Fluorescence

paraformaldehyde was used to fix cells for the preliminary visualisation experiments. The glass coverslips were mounted in the custom imaging chamber discussed in Chapter 7 for light-sheet imaging.

## 8.6 Spell out SPT using SPIM

The secondary optical relay was set to  $2.5 \times$  magnification, giving  $62.5 \times$  at the sample plane, to ensure the camera was Nyquist limited so that there were sufficient pixels available to observe astigmatism on a single particle. The weakly cylindrical lens ( $f = 1$  m) was inserted in between the secondary relay and the camera unit at 40 mm away from the aperture of the camera. The cylindrical lens was inserted in between the camera and the tube lens as adding the cylindrical lens in an infinity space would have amplified the astigmatic effect (to beyond usable), and disabled any tuning of the astigmatism through positioning.

For calibration of the axial particle tracking, an agarose gel of beads was imaged with the objective and the light-sheet synchronously iterated through small axial steps. Moving the stage would have better emulated how a particle would appear, however, the mechanical resolution and hysteresis of the translation stage made this infeasible.

To compare the quality of the calibration, the curves were linearly regressed, see Table 8.1. It was shown that using cross correlation provides a more linear curve calibration. However there is a lower residual sum of squares, meaning co-variance may reduce the error in fitting. As the neither of the calibration curves are obviously

This answered the  
pixel width  
corre ← the  
size of the  
image PSF  
width, so  
that PSF  
width could  
be  
accurately  
estimated.

Give Thompson Equation for reference.

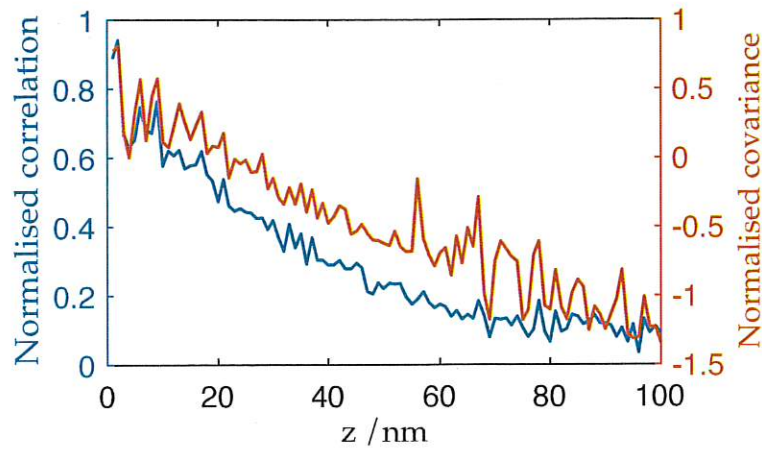


Fig. 8.8 Curves showing calibration between axial depth within the light-sheet and template matched cross-correlation (blue) and covariance (orange)

- 1 linear, a linear regression may not be the best metric for comparison; however, there  
 2 is no model for how the system should respond and so using another function would  
 3 be guess work. Empirically, the calibration curve for correlation looks less variant  
 4 than when using covariance, suggesting a linear fit is not sufficient.

Table 8.1 Table of regressional analysis for calibration curves in Figure 8.8. RSS: Residual sum of squares;  $R^2$ : Coefficient of determination; RMS: Root mean square

Metric	RSS	$R^2$	RMS
Covariance	0.633	0.8569	0.08037
Cross-correlation	2.984	0.8904	0.08037

Be quantitative, if possible,  
*i.e. Linear fit*  
 E.g. estimation using this  
 method had a  
 maximum error of  
 100 nm, and a typical error of 50 nm...

## 8.7 Conclusions

- 6 It was shown that the inverted light-sheet system as described in this work is  
 7 capable of axially localising diffraction-limited particles. This was demonstrated  
 8 experimentally using static sub-diffraction limit particles with a view to applying  
 9 the same techniques to dynamic particles. It was also shown that dynamic particles  
 10 within when tracked astigmatically are susceptible to a localisation error on the order ✓  
 11 of 25 % given standard imaging and biological conditions. This was demonstrated  
 12 on a model system analytically and could be used in other systems for calculations.

numerically

The detection objective used in the light-sheet system was ~~victim to~~ significant spherical aberration. The spherical aberration was addressed using a bespoke tool to manually rotate the correction collar on the objective lens; this then lead to dramatic coma effects which had otherwise been masked by spherical aberration. The latter aberration could not be corrected for which made Gaussian fitting in feasible for axial localisation. However, template-matching techniques did still produce a viable calibration curve that could be used, with cross-correlation being the more reliable reporter.

*R estimator*

*affected by*

*lowest mean square error?*

### 8.7.1 Future work

It was also shown that a Nyquist limited cellular image could also be acquired using this system. By using a CO<sub>2</sub> free buffer, such as HEPES, HeLa could be imaged in this system for long enough to observe viral egress within a live cell. The next step for particle tracking would be to observe single particles diffusing in a viscous medium that acts as an analogue for the cell. Once both of these have been demonstrated, SPT of viral egress from a live cell may be achieved.

## Neural networks

In this work, the techniques presented for localising particles, in an astigmatic system, rely on a singular calibrated point emitter, the template. A population of point-emitters with known axial positions would help mitigate potential axial localisation errors. It is possible to align multiple calibration volumes and create an averaged or model calibration volume to work with, though this method relies heavily on the sub-pixel alignment step to reduce error.

Training a neural network could be a more robust approach. Neural networks take multiple inputs and produce a single output based on a back propagation step which helps determine the weightings on the *neurons* in the hidden layer or layers. Convolutional neural networks work in a similar fashion except that the weightings are image convolution steps; by using convolution steps the overall size of the neural network needed reduces making image recognition possible. By training a neural network on a given input segmented input image, with the known output of axial position, a fast and accurate machine for producing axial localisations could be utilised. Neural networks are also computationally inexpensive as most of the effort put in occurs during the training step.

*NOT  
REALLY  
CONVINCED.  
MAKE  
A  
FIGURE IF  
YOU WANT  
TO SUBMIT  
THIS  
APPROACH.*

Draft - v1.0

Friday 1<sup>st</sup> June, 2018 - 17:50